Parametric Study of Federated Conflict Resolution for UAM Operations

Min Xue*
NASA Ames Research Center, Moffett Field, CA 94035

Matthew Kowalski†
NASA Langley Research Center, Hampton, VA 23666

This work presents a federated conflict resolution algorithm and its parametric study for UAM operations. A federated speed-control-based conflict resolution algorithm is introduced first, including its rules of the road, data exchange requirement, and critical parameters. Two experiments were set up for the parametric study. The first investigates five parameters: look ahead time, resolution update interval, maximum allowed speed reduction, traffic flow interval, and crossing angle. The second experiment studies the uncertainty of departure time. Metrics associated with safety, efficiency, and conflict resolution effort were measured for each scenario. A Design Of Experiment (DOE) analysis was used to perform the multi-factor analysis for the first experiment. It revealed that the crossing angle and flow interval were the most critical parameters across all three metrics, followed by maximum allowed speed reduction. Look ahead time and resolution update interval were of minor significance to safety and conflict resolution effort, but had little to no effect on efficiency. The analysis of the second experiment showed that, given a flow rate, the fluctuation in departure time was absorbed by the conflict resolution algorithm, which resulted in a relatively small fluctuation in airborne delay.

I. Introduction

To support the development of a safe, efficient, and scalable Urban Air Mobility (UAM) ecosystem, the Federal Aviation Administration (FAA) published the first version of UAM concept of operations [1] with the support from NASA and industry partners. According to the ConOps, a federated autonomous system that consists of Providers of Services for UAM (PSU) network will be utilized by operators for UAM operations. The FAA will set UAM corridors based on operational design. The separation within the corridors will be allocated to the UAM operators with the support from the PSUs and will follow the Community Based Rules (CBRs) approved by the FAA. To understand the federated conflict resolution in UAM corridor operations, a study of the function is necessary.

In past decades, rules have been developed and utilized in different ways by the conflict resolution algorithms for guiding and/or coordinating resolution maneuvers between aircraft. These rules include, but are not limited to, the protocol based method [2], the fuzzy logic based method [3], the partially observable Markov decision process method [4], and the logic table based Traffic Alert and Collision Avoidance System (TCAS) [5] and Airborne Collision Avoidance System X (ACAS-X) [6]. The rules in these algorithms were developed for specific applications, such as conventional aviation or small UAV operations. Because of the potential difference in vehicle performance and operational environments, rules suitable for UAM corridor operations need to be developed, and parameters in the conflict resolution algorithms must be investigated.

The scope of this work is to study rules and parameters that define a federated conflict resolution algorithm, which will be used in corridor operations as assumed in the ConOps. Due to the relative simplicity of corridor operations, this work concentrates on the parametric study and investigates the impact of these parameter settings on the safety and efficiency of UAM operations. Scenarios with two crossing single-lane corridors are constructed. This study starts with the data exchange required by the federated conflict resolution algorithm, then it proposes the rules of the road (or CBRs) needed for the specific scenarios. The critical parameters that are typically used in most conflict resolution algorithms are then introduced. Statistical analyses are conducted based on the simulation results to reveal the impact of various parameters on the airspace system in terms of safety, efficiency, and conflict resolution effort, which is measured by the number of maneuvers.

*Aerospace Research Engineer, Aviation Systems Division. Mail Stop 210-15. AIAA senior member.
†Statistical Engineer, Systems Engineering Engineering Methods Branch. Mail Stop 290. AIAA member.

This paper is organized as follows: Section II introduces the federated conflict resolution algorithm including its data requirement, rules of the road, and critical parameters. Section III describes two sets of experiments used for this study. Section IV describes the Design of Experiments (DOE) analysis method. Section V presents parametric study results, and Section VI concludes this work.

II. Federated Conflict Resolution

If there are N aircraft operating in an area, a conflict resolution algorithm will be referred to as "centralized" if it manages all N aircraft in the same area. As a comparison, a "federated" conflict resolution will only manage n aircraft, with $n < N$, and leave the rest $(N - n)$ aircraft managed by other federated conflict resolution algorithm(s). The extreme situation would be $n = 1$, where each aircraft has its own conflict resolution algorithm or service. Therefore, data sharing and standardized rules and resolution parameters are critical for "federated" conflict resolution algorithms cooperating with each other. Without loss of generality, this work investigates the extreme case of a "federated" conflict resolution algorithm with $n = 1$.

A. Required Data Exchange

The federated conflict resolution algorithm in this study requires each aircraft to share its current location, velocity, and flight plan (3D waypoints and desired ground speeds) every half second (as shown in Fig. 1). The data is assumed to be shared either through vehicle to vehicle communication, or through ground-based services. No latency is assumed for data sharing, although it can be incorporated and studied in future work. When one aircraft updates its flight plan, the updated information (shown as yellow and orange fonts in Fig. 1) will be broadcast to the neighboring aircraft next time step.

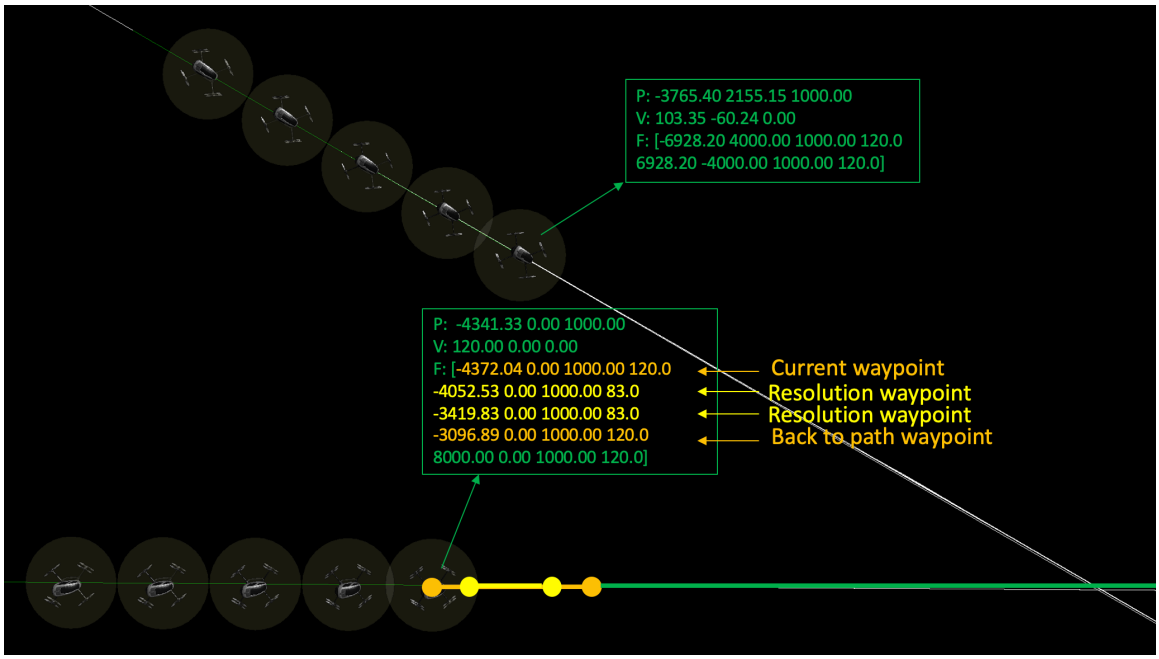

Fig. 1 Data sharing in the federated conflict resolution algorithm

B. Conflict Resolution Procedure

Figure 2 presents the flow diagram of the federated conflict resolution. It starts from its own flight plan and is followed by trajectory generation. Then the aircraft broadcasts its own data (or via its conflict resolution service provider) and receives the data from surrounding aircraft (or through their service providers). The aircraft (or its conflict resolution service provider) then decides if there is any conflict. If yes, the algorithm/service will apply predefined standardized rules and parameters to compute an updated flight plan, which will be then used next time step.

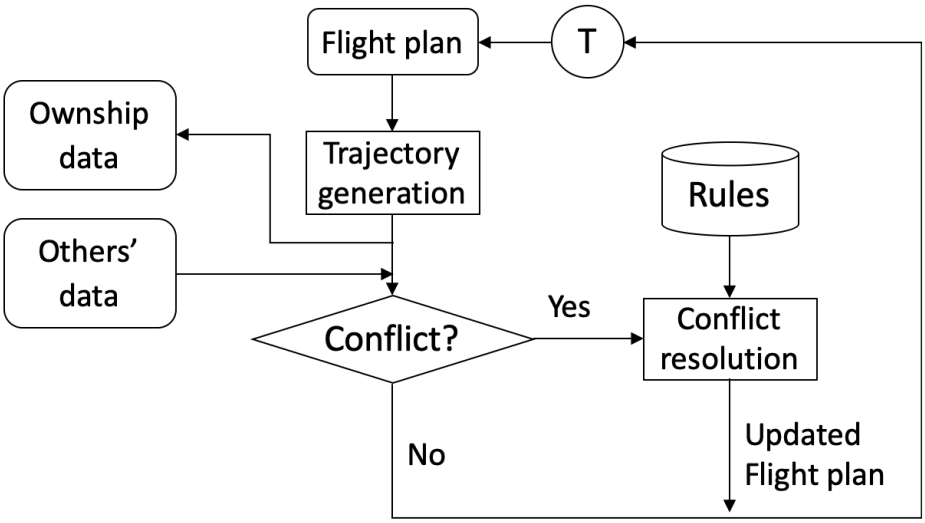

Fig. 2 Flow diagram of the federated conflict resolution algorithm

C. Rules

Rules or decision logic are the core of a conflict resolution algorithm. Some algorithms [2, 3, 7] use the "if-then" statements. Others use tables [5, 6] or even neural networks [8, 9]. As this work concentrates on the resolution parameters and speed change is the only option used for resolutions, the rules are simply defined as follows:

- If the ownship arrives at the crossing point later than an intruder, the ownship is responsible to take action to avoid potential conflict with the intruder.
- Tie-breaker: If both the ownship and intruder arrive at the crossing point at the same time, the vehicle that is on the right side has the right of way.

The first rule is applied for resolving conflict between two traffic flows when they have conflicts at the crossing point. It can also help resolve conflicts between flights in the same traffic flow: when the front flight is adjusting speed, the trailing flight can use the same rule to avoid potential conflict with the front flight. The second rule is added as a tie-breaker when two aircraft have the same (or very close) arrival time at the crossing point. Experiments in this work found the tie breaker is necessary.

D. Resolution parameters

In a conflict resolution algorithm, there are several parameters that can be critical to the resolution algorithm performance. This work investigates the following key parameters:

- Look ahead time: This parameter is defined as the time threshold when a resolution action should be taken to avoid conflict. A proper resolution time threshold can help avoid unnecessary maneuvers while maintaining safety.
- Resolution update interval: The second parameter is the resolution update interval, which is essentially related to how often a resolution maneuver should be re-evaluated. By default, conflict resolution will be triggered when a potential conflict is predicted to happen in the foreseeable future. Once a conflict resolution maneuver is assigned, it will not be updated unless another potential conflict is predicted to happen. This event-triggered mechanism works fine for providing safety, however, it might not be efficient though. For instance, when the situation evolves and there is a false alarm, the current resolution maneuver may not be efficient or even needed. Having a smaller interval may help improve efficiency.
- Maximum allowed speed reduction: The third parameter is related to the maneuver option - the maximum allowed speed reduction. As proposed UAM vehicles have the capability of flying at a much lower speed or even hovering, it gives the conflict resolution algorithm more options to resolve conflict. However, there will be a trade-off between efficiency and safety. It will be desired to examine the relationship between the maximum allowed speed reduction and system performance, such as safety and efficiency.

III. Experiment Setup

Experiments are conducted using the Fe^3 fast-time simulator [10]. The Fe^3 simulator includes a 6-DOF trajectory model developed based on NASA's UAM concept vehicle [11]. The configurable federated conflict resolution algorithm in the simulator allows parameters to be varied easily, which enables a large number of simulations needed for this work.

To conduct the parametric study for the conflict resolution, route-based scenarios with two flows crossing at various angles were used for experiments to mimic single-lane corridor operations. A federated conflict resolution algorithm is then applied by individual aircraft, as discussed in the previous section. It is assumed to have five flights in each flow and each flight starts with a cruise speed of 120 knots two minutes away from the crossing point, as shown in Fig. 3. An initial flow interval of 10 seconds was imposed between flights and two sets of experiments were conducted in this study.

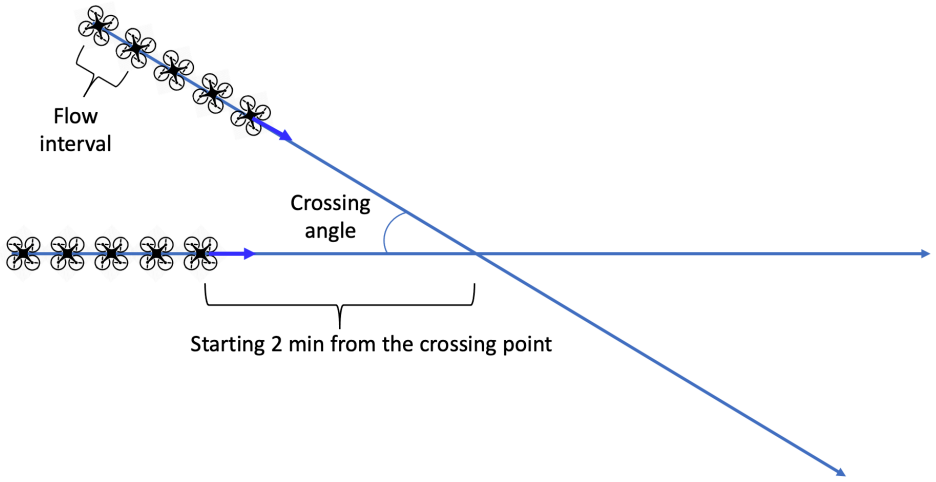

Fig. 3 Experiment scenario notional graph

In the first set of experiments, two flows had fixed departure or starting times. However, parameter settings were varied. Table 1 presents independent variables used in the experiments: look ahead time, resolution update interval, maximum allowed speed reduction, flow interval, and flow crossing angle. The flow interval and crossing angle are external variables, whereas the remaining three are internal conflict resolution parameters. A total of 5,760 scenarios were generated.

Table 1 Independent variables

Independent variable	Value in Experiment 1	Value in Experiment 2	Unit
Look ahead time	60, 90, and 120	60	second
Resolution update interval	1, 2, 5, and 10	1	second
Maximum allowed speed reduction	20, 30, and 50	50	mps
Flow interval	10, 15, 20, 25, and 30	10	second
Flow crossing angle	$[10°, 160°] \cup [200°, 350°]$ with an increment of 10°	30°	degree
Departure time change	0	Poisson(λ=100)	second

The second set of experiments were conducted to study the sensitivity to the difference of starting/departure times between these two flows. In this set of experiments, the starting time of the first flight in one flow was perturbed with a Poisson distribution (shown in Fig. 4) where the distribution parameter λ was set to 100 and most departure delays were assumed between -40 and 40 seconds. The blue curve shows the sampling delays (with a total of 1,000 sampling points). In the second set of experiments, the look ahead time, resolution update interval, maximum allowed speed reduction, flow crossing angle, and flow interval were set to 60 seconds, one second, 50 mps, 30 degrees, and 10 seconds,

respectively.

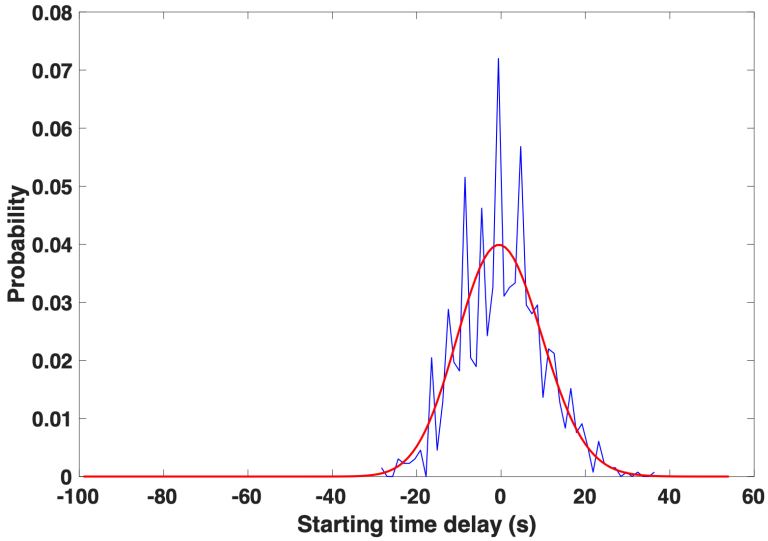

Fig. 4 Starting time delays used in the second experiment

In both sets of experiments, three output metrics are used for safety and efficiency: (1) number of losses of separation, (2) airborne delay, and (3) number of resolution maneuvers. A loss of separation is defined as a violation of the minimum allowed separation of 1,000 ft. The airborne delay is the extra flight time compared to the unimpeded flight time, and the number of resolution maneuvers is simply the count of conflict resolution maneuver commands that were issued. If the resolution interval is one second, the resolution maneuver will be evaluated every second, therefore, the number of resolution maneuvers is also related to the duration of the resolution.

IV. DOE Analysis Method

To reveal the relationships between an input and an output, the best approach is to change the former and see whether the latter changes. When there is more than one input (i.e. factor), a design that changes just one factor at a time is inefficient. Design of experiments, or DOE [12], is an efficient and prevailing approach for exploring multi-factor opportunity spaces. DOE methodologies were originated in studies involving empirical data [13]. However, in recent years, they have been quite successful in helping to gain insight into simulation data [14, 15]. The statistical analysis embedded in the construction of the surrogate model serves as an objective guide to researchers with respect to identifying which variables in their simulation are of importance, and often more critical, which variables interact with one another. The DOE surrogate model can be rapidly queried to answer questions both general and specific pertaining to the research in a much more robust manner than other methods such as the previously mentioned one factor at a time experimentation.

The statistical models in the DOE are essentially a Taylor series expansion, in which each of the independent variables and their interactions serve as model terms along with any non-linear terms such as quadratics or cubics. A statistical test is performed on each model term to determine how much of the residual model error is reduced by inserting that term i.e. effect size (coefficient) into the model. If a term is deemed statistically significant then it remains in the model, otherwise it is removed. A prediction model is generated, which is essentially a multidimensional curve fit through the data in which each independent variable serves as a dimension.

The analysis of the first set of experiments involved methodologies associated with the DOE method. At the beginning of the analysis for each of the dependent variables, a comprehensive starting model was chosen, where statistically significant model terms were kept and insignificant terms were removed. The first experiment provided a test matrix comprised of $(3 \times 4 \times 3 \times 5 \times 32) = 5,760$ runs . Because every combination was run in this experiment, all five variables along with all possible interactions between them: from a pairwise two-factor interaction (2FI) all the way up to a five-factor interaction (5FI) can be evaluated simultaneously using DOE. In this work, 75 variable relationships, including the five variables and selected combinations of these variables, were used as the starting model terms. The rich data generated by the first experiment helps identify and quantify variable interactions/dependencies among the

parameters internal and external to the federated conflict resolution algorithm, which is the key to understanding and developing meaningful UAM operations.

Of importance to note are that the independent variable of crossing angle in degrees introduces a different type of coordinate system than that of the other four variables. This makes statistical modeling problematic because both Cartesian and Polar coordinate systems are being considered in the statistical sampling (i.e. test matrix). This was addressed by inserting higher-order nonlinear model terms. For example: to fit a line requires two settings, to fit a quadratic requires three, and so on and so forth. The 34 increments along the crossing angle variable allow for a high degree of curvature to be modeled. This curvature modeling capability helps compensate for the circular nature of the polar coordinate system.

Different modeling types were used in this study to address the differences in the mathematical properties of each of the dependent response outputs. Safety was measured by a count of the number of losses of separation in each of the run scenarios. Count data can be difficult to analyze because it is categorical in nature, particularly if the range of counts is small. If both instances are true (as they are in this case) then the data set provides limited granularity to detect differences as a function of independent variable settings. Count data is typically distributed according to a Poisson distribution. Thus, the appropriate statistical modeling for this type of data is the Generalized Linear Model (GLM) with a Poisson distribution (as shown in Table 2). The second output metric - the sensitivity of efficiency - was quantified by a measure of the extra flight time induced by airborne delays in seconds for each of the run scenarios produced. This dependent variable is continuous in nature. Thus, the statistical modeling for this type of data is the Response Surface Methodology (RSM), which assumes a Normal distribution. The sensitivity of conflict resolution effort was quantified by a count of the amount of times the algorithm had to issue a conflict resolution maneuver to any of the UAMs in flight. This dependent variable is categorical in nature just like the number of losses of separation. Thus, the Generalized Linear Model (GLM) with a Poisson distribution was used for the analysis. Table 2 illustrates the modeling used for each output.

Table 2 Output metrics

Dependent variable	Category	Unit	Modeling type	Distribution	Link function
Number of losses of separation	Safety	1	GLM	Poisson	Log
Airborne delay	Efficiency	second	RSM	Normal	NA
Number of resolution maneuvers	Efficiency	1	GLM	Poisson	Log

V. Results

The sensitivity of safety, efficiency, and conflict resolution effort to the aforementioned parameters (look ahead time, resolution update interval, maximum allowed speed reduction, flow interval, flow crossing angle, and departure time variation) are analyzed in this section. The first three subsections cover the analysis of the first experiment using the DOE method. For the second set of experiments, the sensitivity to the departure delay is analyzed separately and presented in the final subsection.

A. Safety

The table in Fig. 5 lists the statistically significant model terms from the 75 starting model terms discussed previously. Notice the p-values of each of the model terms are well below five significant digits in terms of their size. A LogWorth transform is used on the p-values in order to make better comparisons between them. The LogWorth transform is simply –log10(p-value). Important to note is that the effect summary in the table only speaks to statistical significance and not necessarily the effect sizes themselves. This is a limitation of using the GLM to model the data. The RSM modeling of the next dependent variable does not have this limitation. As shown in the table, the independent variables of X4 (flow interval) and X5 (crossing angle) are of high statistical significance along with their two-factor interaction. X3: Maximum Allowed Speed reduction is of interest as well as it appears in several interactions. All original five independent variables were of statistical significance either on their own or involved in an interaction.

In order to aid in the interpretation of this multidimensional model, the JMP® tool [16] is used to generate the factor profiler, which is essentially a series of two-dimensional projections through the multidimensional input/output space.

Model Term	LogWorth	LogWorth (graph)	p-value
X4: Flow Interval/Separation	248.759		0.00000
X5: Crossing Angle (symmetric)	105.161		0.00000
X4: Flow Interval/Separation*X5: Crossing Angle (symmetric)	79.983		0.00000
X5: Crossing Angle (symmetric)*X5: Crossing Angle (symmetric)*X3: Maximum Allowed Speed Reduction (mps)	47.648		0.00000
X1: Look Ahead Time*X3: Maximum Allowed Speed Reduction (mps)*X5: Crossing Angle (symmetric)	31.887		0.00000
X1: Look Ahead Time*X3: Maximum Allowed Speed Reduction (mps)	27.756		0.00000
X3: Maximum Allowed Speed Reduction (mps)*X4: Flow Interval/Separation	22.496		0.00000
X2: Resolution Update Interval	16.758		0.00000
X5: Crossing Angle (symmetric)*X5: Crossing Angle (symmetric)	16.105		0.00000
X3: Maximum Allowed Speed Reduction (mps)*X5: Crossing Angle (symmetric)	13.198		0.00000
X5: Crossing Angle (symmetric)*X5: Crossing Angle (symmetric)*X5: Crossing Angle (symmetric)	9.193		0.00000
X3: Maximum Allowed Speed Reduction (mps)	8.741		0.00000
X1: Look Ahead Time*X5: Crossing Angle (symmetric)	7.192		0.00000
X1: Look Ahead Time	5.481		0.00000

Fig. 5 Effect summary for the number of losses of separation

Fig.6 illustrates how the model behaves based on the independent variable settings. The dashed red lines with each plot show the least safe settings (when the number of losses of separation is the highest) according to the model, which is when the look ahead time is low, resolution update interval is high, maximum allowed speed reduction is low, flow interval is low, and crossing angle is 120 degrees.

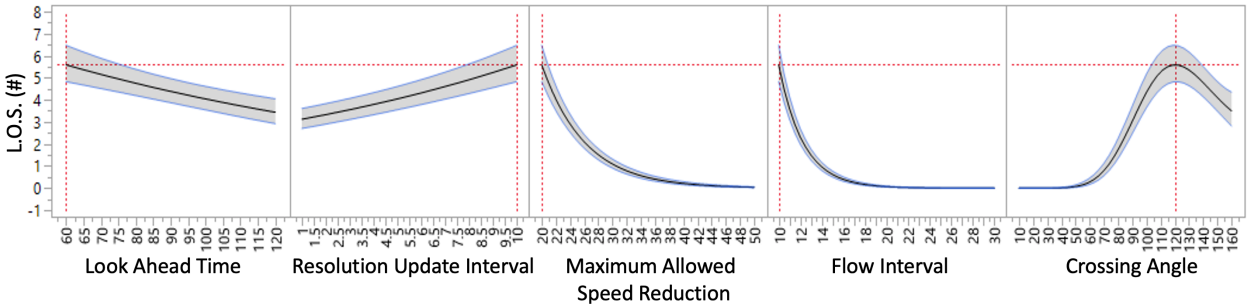

Fig. 6 Profiler for the maximum number of losses of separation

Figure 7 further explores the essentially unsafe regions of the input space in the form of a series of both 3D surface plots and 2D contour plots. It is worthwhile to mention that the statistical model discussed may not be a perfect fit through the data because of the nature of the dependent variable as count data. However, it is adequate to use the method to identify which model terms are most influential and which areas of the input space i.e. independent variable settings are either desirable or undesirable. Figures 7(a) and 7(b) show the 3D plots when the X5 (crossing angle) was held along the X axis and the other two independent variables X1 (look ahead time) and X3 (maximum allowed speed reduction) are plotted along the horizontal axis for comparison, respectively. The vertical axis denotes the projected number of losses of separations. When not shown in any particular plot, the remaining independent variables were kept at their "worst-case" settings that are essentially the settings listed in Fig. 6. Figures 7(c) and 7(d) show the corresponding 2D contour plots, where the dark red color represent the unsafe region.

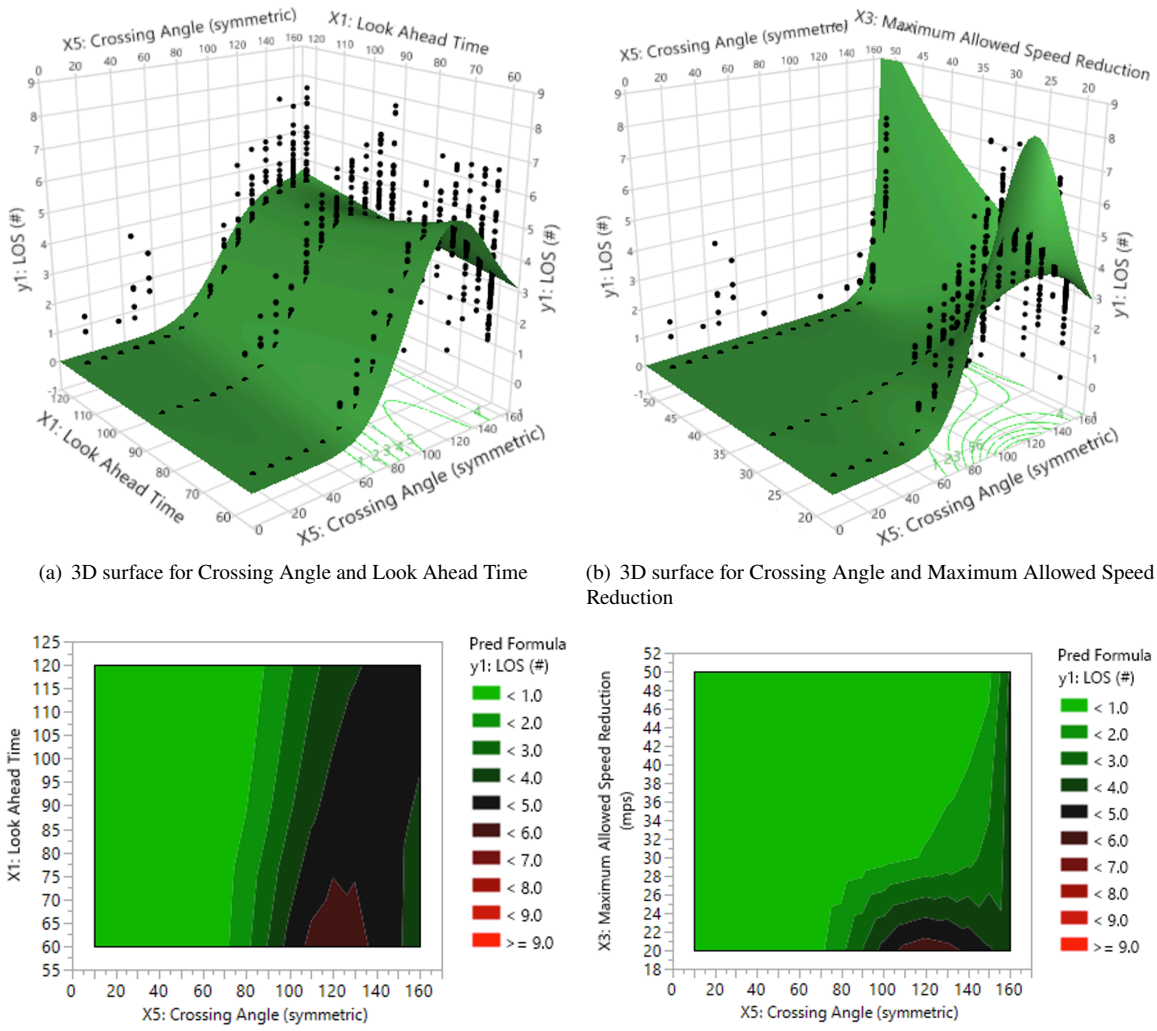

(a) 3D surface for Crossing Angle and Look Ahead Time

(b) 3D surface for Crossing Angle and Maximum Allowed Speed Reduction

(c) 2D contour for Crossing Angle and Look Ahead Time

(d) 2D contour for Crossing Angle and Maximum Allowed Speed Reduction

Fig. 7 3D surface and 2D contour for the maximum number of losses of separation

B. Efficiency

Figure 8 lists the statistically significant model terms, which remained from the original 75 in the starting model for efficiency. Efficiency is measured by the extra flight time induced by airborne delays in seconds for each of the run scenarios produced. Notice the p-values of each of the model terms are well below four significant digits in terms of their size. Important to note is that the scaled estimates table below does reflect the relative effect sizes as they have all been scaled according to the ranges of the independent variables from the data. Blue is for a positive effect (from low to high input settings) and red is for a negative effect (from low to high input settings). As shown in the figure, the independent variable X5 (crossing angle) has many non-linear terms denoted by it being crossed with itself several times in the table. X4 (flow interval) is significant along with various linear and non-linear interactions with X5 (crossing angle). X3 (maximum allowed speed reduction) is of minor interest as well as it appears in several less significant interactions. Interesting to note is that independent variables X1 (resolution update interval) and X2 (look ahead time) were not of importance with respect to airborne delay. Statistically, they were removed from the model but manually reinserted for comparison's sake.

As before, the Factor Profiler generated by the JMP® tool is used to illustrate features of the model graphically. Fig. 9 shows that the highest prediction airborne delay (least efficient) is when the look ahead time is low, resolution

Term	Scaled Estimate	Scaled Estimate (graph)	p-value
Intercept	69.334		<.0001
(X5: Crossing Angle (symmetric))*(X5: Crossing Angle (symmetric))	338.309		<.0001
(X5: Crossing Angle (symmetric))*(X5: Crossing Angle (symmetric))*(X5: Crossing Angle (symmetric))	302.121		<.0001
(X4: Flow Interval/Separation)*(X5: Crossing Angle (symmetric))	-189.220		<.0001
(X5: Crossing Angle (symmetric))*(X5: Crossing Angle (symmetric))*(X5: Crossing Angle (symmetric))*(X4: Flow Interval/Separation)	164.686		<.0001
X4: Flow Interval/Separation	-98.135		<.0001
X5: Crossing Angle (symmetric)	80.047		<.0001
(X5: Crossing Angle (symmetric))*(X5: Crossing Angle (symmetric))*(X3: Maximum Allowed Speed Reduction (mps))	-50.372		<.0001
(X3: Maximum Allowed Speed Reduction (mps))*(X5: Crossing Angle (symmetric))	-46.466		<.0001
(X3: Maximum Allowed Speed Reduction (mps))*(X4: Flow Interval/Separation)*(X5: Crossing Angle (symmetric))	21.802		<.0001
X2: Resolution Update Interval	5.689		0.0103
X1: Look Ahead Time	-0.752		0.7216

Fig. 8 Scaled estimates for airborne delays

update interval is high, maximum allowed speed reduction is low, flow interval is low, and crossing angle is high.

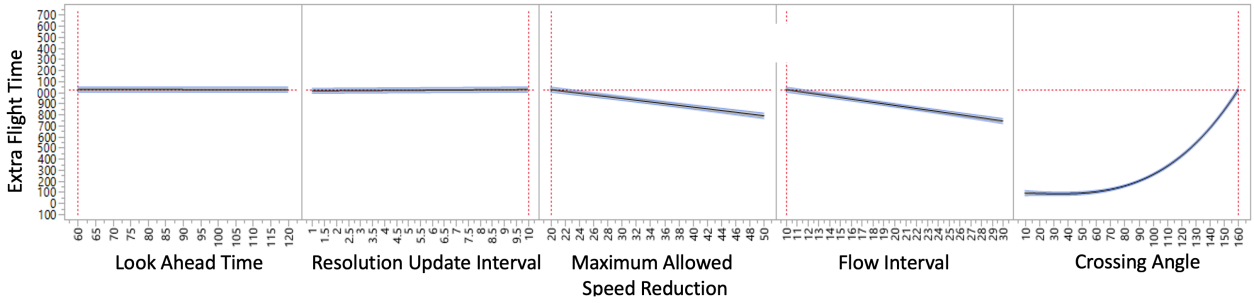

Fig. 9 Profiler for the maximum airborne delays

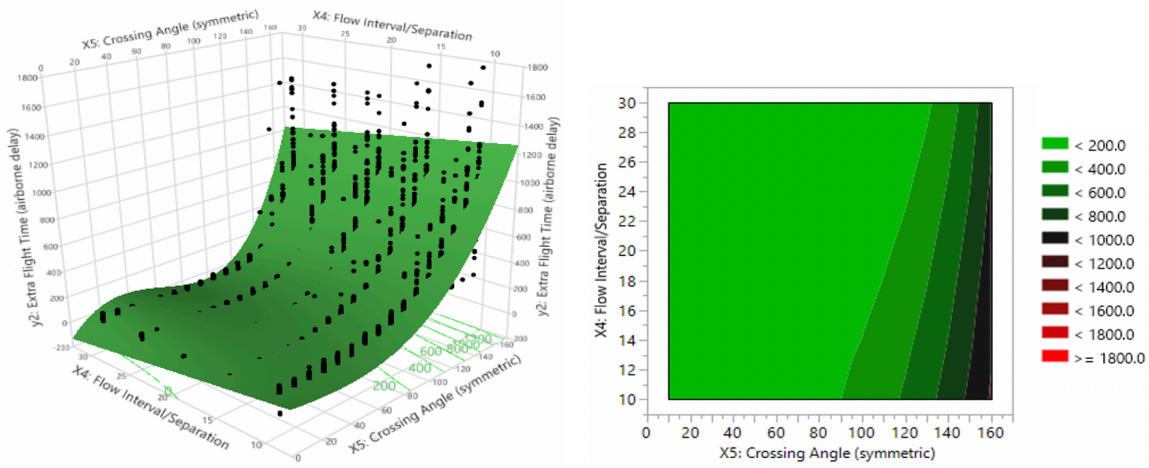

(a) 3D surface for Crossing Angle and Flow Interval

(b) 2D contour for Crossing Angle and Flow Interval

Fig. 10 3D surface and 2D contour for the maximum airborne delays

Figure 10 explores the essentially inefficient regions of the input space using both 3D surface plots and 2D contour plots. Again, when not shown in any particular plot, the remaining independent variables were kept at their "worst-case" settings that are essentially the settings listed in Fig. 9. In Fig. 10(a), the two horizontal axes are X5 (crossing angle) and X4 (flow interval) and the vertical axis denotes the airborne delay, and in Fig. 10(b) the darker shades of green represent increased airborne delay. Fig. 10(b) shows that crossing angles less than 90 degrees exhibit little to no airborne delay if the flow interval is greater than 10 seconds. It implies that most merging scenarios (i.e. crossing angles < 90 degrees)

should expect to see no delays if the flow interval is more than 10 seconds. However, delays start to become more likely when crossing angles are beyond 90 degrees, which is when merging scenarios transition to head-on scenarios. The most relevant independent variable to manipulate would be the flow interval as the other variables have little to no effect on airborne delays. This mitigation also has implications on the route structure design and identifies characteristics to avoid and how to mitigate them if they cannot be avoided.

C. Conflict Resolution Effort

Figure 11 lists the statistically significant model terms for the total number of conflict resolution maneuvers to all flights. Notice the p-values of each of the model terms are well below five significant digits in terms of their size. The GLM model was used due to the nature of the count data. As shown in the figure, the independent variable X4 (flow interval), X5 (crossing angle), and X3 (maximum allowed speed reduction) all had a significant effect on the model. Non-linear effects associated with X5 (crossing angle) appeared as well along with several linear and non-linear interactions. In this case X1 (look ahead time) seemed to have the least significance.

Model Term	LogWorth	LogWorth (graph)	p-value
X4: Flow Interval/Separation	46327.52		0.00000
X5: Crossing Angle (symmetric)	22200.49		0.00000
X3: Maximum Allowed Speed Reduction (mps)	19636.77		0.00000
X5: Crossing Angle (symmetric)*X5: Crossing Angle (symmetric)	9535.954		0.00000
X5: Crossing Angle (symmetric)*X5: Crossing Angle (symmetric)*X4: Flow Interval/Separation	5819.591		0.00000
X2: Resolution Update Interval	3987.561		0.00000
X2: Resolution Update Interval*X3: Maximum Allowed Speed Reduction (mps)	3248.1		0.00000
X5: Crossing Angle (symmetric)*X5: Crossing Angle (symmetric)*X3: Maximum Allowed Speed Reduction (mps)	2113.51		0.00000
X5: Crossing Angle (symmetric)*X5: Crossing Angle (symmetric)*X5: Crossing Angle (symmetric)*X4: Flow Interval/Separation	1660.353		0.00000
X5: Crossing Angle (symmetric)*X5: Crossing Angle (symmetric)*X2: Resolution Update Interval	779.276		0.00000
X5: Crossing Angle (symmetric)*X5: Crossing Angle (symmetric)*X5: Crossing Angle (symmetric)*X2: Resolution Update Interval	594.062		0.00000
X3: Maximum Allowed Speed Reduction (mps)*X5: Crossing Angle (symmetric)	465.716		0.00000
X1: Look Ahead Time	448.395		0.00000
X3: Maximum Allowed Speed Reduction (mps)*X4: Flow Interval/Separation	340.947		0.00000
X2: Resolution Update Interval*X3: Maximum Allowed Speed Reduction (mps)*X4: Flow Interval/Separation*X5: Crossing Angle (symmetric)	236.913		0.00000
X3: Maximum Allowed Speed Reduction (mps)*X4: Flow Interval/Separation*X5: Crossing Angle (symmetric)	225.656		0.00000
X5: Crossing Angle (symmetric)*X5: Crossing Angle (symmetric)*X5: Crossing Angle (symmetric)*X3: Maximum Allowed Speed Reduction (mps)	152.796		0.00000
X2: Resolution Update Interval*X4: Flow Interval/Separation	114.611		0.00000
X1: Look Ahead Time*X5: Crossing Angle (symmetric)	100.872		0.00000
X2: Resolution Update Interval*X5: Crossing Angle (symmetric)	79.185		0.00000
X1: Look Ahead Time*X3: Maximum Allowed Speed Reduction (mps)	67.036		0.00000
X2: Resolution Update Interval*X3: Maximum Allowed Speed Reduction (mps)*X5: Crossing Angle (symmetric)	57.359		0.00000
X1: Look Ahead Time*X3: Maximum Allowed Speed Reduction (mps)*X4: Flow Interval/Separation*X5: Crossing Angle (symmetric)	53.24		0.00000
X1: Look Ahead Time*X2: Resolution Update Interval	50.395		0.00000
X1: Look Ahead Time*X3: Maximum Allowed Speed Reduction (mps)*X4: Flow Interval/Separation	41.965		0.00000
X5: Crossing Angle (symmetric)*X5: Crossing Angle (symmetric)*X5: Crossing Angle (symmetric)*X1: Look Ahead Time	39.053		0.00000
X5: Crossing Angle (symmetric)*X5: Crossing Angle (symmetric)*X5: Crossing Angle (symmetric)	37.361		0.00000
X1: Look Ahead Time*X2: Resolution Update Interval*X3: Maximum Allowed Speed Reduction (mps)*X4: Flow Interval/Separation	35.326		0.00000
X1: Look Ahead Time*X2: Resolution Update Interval*X3: Maximum Allowed Speed Reduction (mps)	28.13		0.00000
X2: Resolution Update Interval*X3: Maximum Allowed Speed Reduction (mps)*X4: Flow Interval/Separation	21.536		0.00000
X5: Crossing Angle (symmetric)*X5: Crossing Angle (symmetric)*X1: Look Ahead Time	18.347		0.00000
X1: Look Ahead Time*X2: Resolution Update Interval*X4: Flow Interval/Separation*X5: Crossing Angle (symmetric)	12.99		0.00000
X1: Look Ahead Time*X2: Resolution Update Interval*X3: Maximum Allowed Speed Reduction (mps)*X4: Flow Interval/Separation*X5: Crossing Angle (symmetric)	8.107		0.00000
X1: Look Ahead Time*X4: Flow Interval/Separation*X5: Crossing Angle (symmetric)	6.465		0.00000

Fig. 11 Effect summary for the number of conflict resolution maneuvers

As with the previous two models, the Factor Profiler generated by the JMP® tool is used to illustrate features of the model graphically. Fig. 12 shows that the highest prediction of conflict resolution maneuvers is when look ahead time is high, resolution update interval is high, maximum allowed speed reduction is low, flow interval is low, and crossing angle is high.

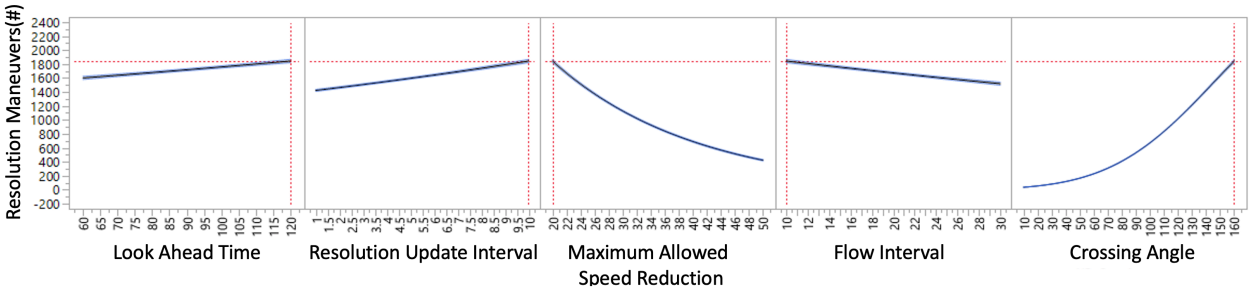

Fig. 12 Profiler for the maximum number of conflict resolution maneuvers

Figure 13 presents the regions of the maximum amount of conflict resolution maneuvers. In Fig. 13(a), the vertical axis denotes the number of conflict resolution maneuvers, and the two inputs with the horizontal axes are crossing angle and maximum allowed speed reduction. Recall that when not shown in any particular plot, the remaining independent variables were kept at their "worst-case" settings that are essentially the settings listed in Fig. 12. In Fig. 13(b) the green to red color gradient represents increasing numbers of conflict resolution maneuvers.

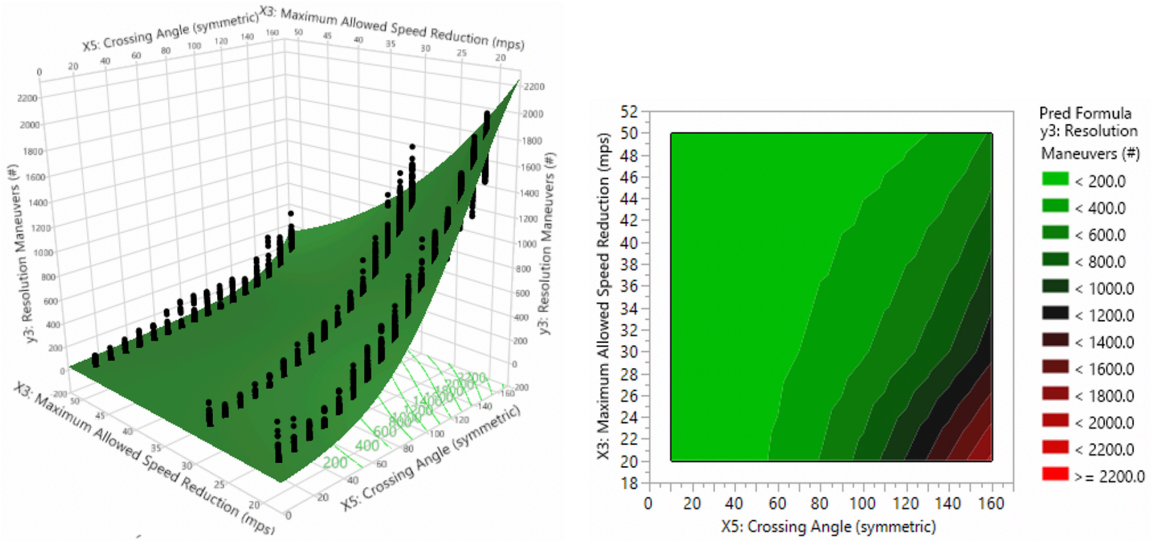

(a) 3D surface for crossing angle and max. allowed speed reduction (b) 2D contour for crossing angle and max. allowed speed reduction

Fig. 13 3D surface and 2D contour for the maximum number of conflict resolution maneuvers

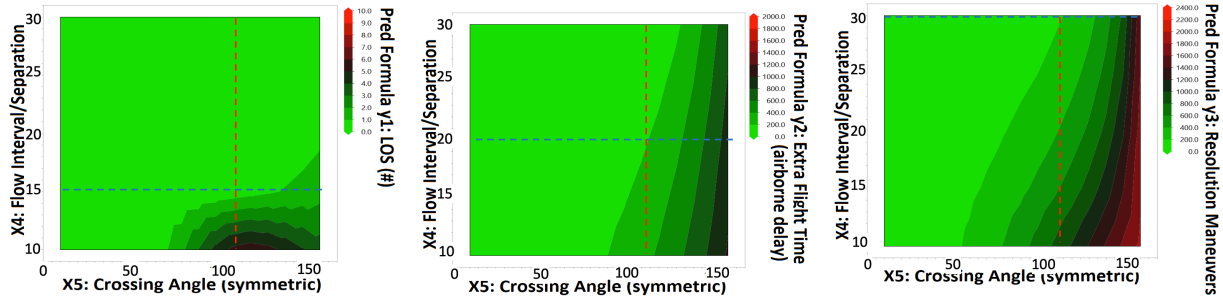

(a) Design space for safety (b) Design space for efficiency (c) Design space for resolution effort

Fig. 14 Example of defining requirements across multiple output metrics

Figure 14 combines the results of all three of the output variables in order to exploit an inherent benefit of measuring and modeling multiple outputs of a designed experiment. Due to the fact that the data for all three output variables was sampled across the same input space; comparisons between the different models can be made by simply stacking the input space, as is shown in Fig. 14. In this instance the X4 (flow interval) and X5 (crossing angle) dimensions were chosen because they were the most influential across all three output variables. The red dotted line denotes a crossing angle of 110 degrees to provide an example of a problematic route structure and how it could be mitigated across all three output variables simultaneously. The contour plot in Fig. 14(a) illustrates that a flow interval of 15s or higher would mitigate losses of separation. The middle contour plot in Fig. 14(b) indicates that a flow interval of 20s or higher would minimize extra flight time delay. The contour plot in Fig. 14(c) shows that the maximum value of 30s or higher is needed in order to minimize resolution maneuvers. Thus, if a requirement was to be written to address the concerns

of all three outputs it would state something to the effect that crossing angles at or around 110 degrees require a flow interval of 30s or higher in order to minimize losses of separation, extra flight time delay, and resolution maneuvers. Of course, different weights can be put on these three outputs, which may result in a different requirement.

The intent of this example is not to impose any implied requirements on crossing angles but rather to illustrate how requirements in the future could be written to address multiple output responses using this notion of sampling across a common domain space and then stacking the predictive surrogate models associated with each of the outputs. This allows researchers and other stakeholders to make global decisions across a vast domain space, which may involve many complex dependencies and have visibility into how restrictions on one output metric affect the others.

D. Sensitivity to Departure Delay

When there is uncertainty in departure delay, to examine the system performance using these three output metrics, the second set of experiments with Monte Carlo simulations were conducted. In this experiment, the departure delays were set to follow a Poisson distribution. For the system safety metric, experiment results show that no losses of separation were observed in these 1,000 Monte Carlo runs.

For the system efficiency metric, Fig. 15(a) shows the distribution of the resulting airborne delays. With the proposed federated conflict resolution algorithm, the distribution of airborne delays is quite different from the initial Poisson distribution and they are well managed within a narrow band. The majority of delays are between 100s and 110s (60%) and another 30% are located between 115 and 125 s with only 6-7% left around 140s.

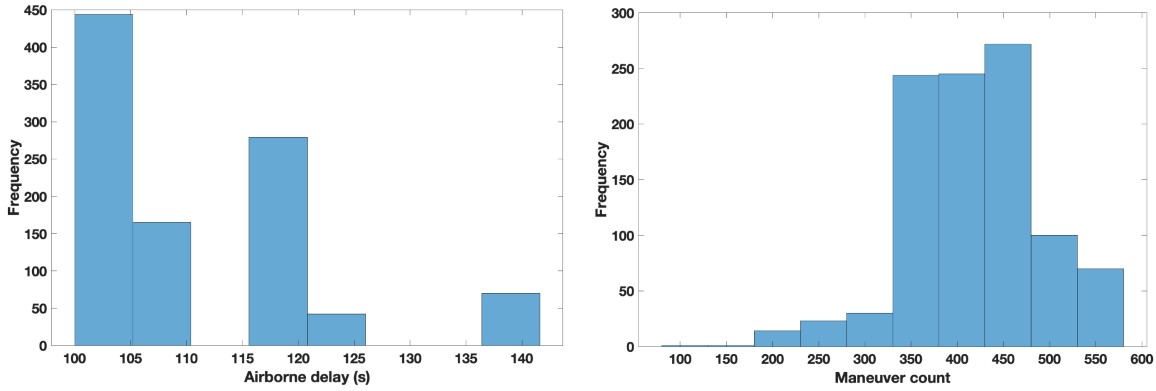

(a) Airborne delay

(b) Number of Maneuvers

Fig. 15 Impact of departure delay with Poisson distribution

For the third conflict resolution metric, Fig. 15(b) presents the distribution of the number of maneuvers, which spreads from 200 to 600. The maneuver count varies from 325 to 475 for the majority of the simulation runs (about 75%). This Poisson or Gaussian-like distribution indicates that the variation caused by departure delays is mostly absorbed by the conflict resolution algorithm, which yields relatively stable airborne delay.

VI. Conclusions

A federated autonomous system consists of Providers of Services for UAM (PSU) network and is expected to be utilized by operators for UAM operations according to the UAM concept of operations published by the FAA. With the FAA setting UAM corridors based on operational design, the separation within the corridors will be allocated to the UAM operators following the Community Based Rules (CBRs) approved by the FAA. A parametric study was conducted to gain in-depth understanding of the federated conflict resolution function in the UAM corridor operations.

A federated algorithm was introduced, including rules of the road, data exchange requirement, and parameters. To explore the parameters and rules needed by a federated tactical separation, two experiments were conducted, where scenarios with two single-lane corridors crossing at different angles were used. The first one investigated five parameters: look ahead time, resolution update intervals, maximum allowed speed reduction, and two parameters external to the conflict resolution algorithm - flow interval and route crossing angle. The DOE method was used for the multi-factor

analysis. The DOE analysis revealed that the crossing angle and flow interval were the most critical parameters across all three metrics, followed by maximum allowed speed reduction. Look ahead time and resolution update interval were of minor significance to safety and conflict resolution effort, but had little to no effect on efficiency. The second experiment was set up to investigate the impact of the uncertainty in departure time. Experiments showed that given a flow rate, the fluctuation in departure time could be absorbed by the conflict resolution algorithm and results in a relatively small fluctuation in airborne delay.

References

[1] *UAM Concept of Operations (ConOps) v1.0*, FAA, 2020. URL `https://www.faa.gov/uas/advanced_operations/urban_air_mobility`.

[2] Hwang, I., and Tomlin, C., "Protocol-based Conflict Resolution for Finite Information Horizon," *Proceedings of the American Control Conference*, Anchorage, AK, 2002.

[3] Cook, B., Cohen, K., and Kivelevitch, E., "A Fuzzy Logic Approach For Low Altitude UAS Traffic Management," *AIAA Science and Technology Forum and Exposition 2016*, San Diego, California, 2016.

[4] Mueller, E., and Kochenderfer, M. J., "Multi-Rotor Aircraft Collision Avoidance using Partially Observable Markov Decision Processes," *AIAA Modeling and Simulation Technologies Conference*, Washington, D.C., 2016.

[5] Kochenderfer, M. J., and Chryssanthacopoulos, J. P., "Robust Airborne Collision Avoidance through Dynamic Programming," Tech. Rep. ATC-371, MIT Lincoln Laboratory, January 2011.

[6] Kochenderfer, M. J., Holland, J. E., and Chryssanthacopoulos, J. P., "Next-Generation Airborne Collision Avoidance System," *Lincoln Laboratory Journal*, Vol. 19, No. 1, 2012, pp. 17–33.

[7] Sislak, D., Volf, P., and Pechoucek, M., "Agent-based Cooperative Decentralized Airplane Collision Avoidance," *IEEE Transactions on Intelligent Transportation Systems*, Vol. 12, No. 1, 2011, pp. 36–46.

[8] Hu, J., Yang, X., Wang, W., Wei, P., Ying, L., and Liu, Y., "UAS Conflict Resolution in Continuous Action Space Using Deep Reniforcement Learning," *AIAA Aviation Forum*, Virtual, 2020.

[9] Das, A., Maratta, K., and Idris, H., "AEGIS: Autonomous Entity Global Intelligence System for Urban Air Mobility," *AIAA Aviation Forum*, Virtual, 2020.

[10] Xue, M., Rios, J., Silva, J., Ishihara, A., and Zhu, Z., "Fe^3: An Evaluation Tool for Low-Altitude Air Traffic Operations," *AIAA Aviation Forum*, Atlanta, GA, 2018.

[11] Silva, C., Johnson, W., Antcliff, K. R., and Patterson, M. D., "VTOL Urban Air Mobility Concept Vehicles for Technology Development," *Aviation Technology, Integration, and Operations Conference*, Atlanta, GA, 2018.

[12] Fisher, R. A., *The Design of Experiments*, Macmillan, 1971.

[13] Montgomery, D. C., *Design and Analysis of Experiments (7th Edition)*, John Wiley & Sons, Inc., 2009.

[14] Myers, R. H., Montgomery, D. C., and Anderson-Cook, C. M., *Response Surface Methodology: Process and Product Optimization Using Designed Experiments, 4th Edition*, Wiley, 2016.

[15] Tolk, A., Diallo, S. Y., Ryzhov, I. O., Yilmaz, L., Buckley, S., and Miller, J. A., "A TUTORIAL ON DESIGN OF EXPERIMENTS FOR SIMULATION MODELING," *Proceedings of the 2014 Winter Simulation Conference*, Tucson, AZ, 2014.

[16] SAS Institute Inc.,, "JMP®," , Version 15.2.1. URL `https://www.jmp.com/`.